Mutations in the *SPTLC1* gene are a cause of amyotrophic lateral sclerosis that may be amenable to serine supplementation

Janel O. Johnson[1,#], Ruth Chia[1,#,*], Ravindran Kumaran[2,#], Nada Alahmady[3,4], Danny E. Miller[5,6], Yevgeniya Abramzon[1,7], Faraz Faghri[8,9], Alan E. Renton[1,10,11], Simon D. Topp[3,12], Hannah A. Pliner[1], J. Raphael Gibbs[13], Jinhui Ding[13], Nathan Smith[2], Natalie Landeck[2], Michael A. Nalls[14], Mark R. Cookson[2], Olga Pletnikova[15], Juan Troncoso[15,16], Sonja W. Scholz[16,17], Marya S. Sabir[17], Sarah Ahmed[17], Clifton L. Dalgard[18,19], Claire Troakes[3], Ashley R. Jones[3], Aleksey Shatunov[3], Alfredo Iacoangeli[3], Ahmad Al Khleifat[3], Nicola Ticozzi[20,21], Vincenzo Silani[20,21], Cinzia Gellera[22], Ian P. Blair[23], Carol Dobson-Stone[24,25], John B. Kwok[24,25], Bryce K. England[26], Emily S. Bonkowski[6], The International ALS Genomics Consortium; The ITALSGEN Consortium; The FALS Sequencing Consortium; The American Genome Center; Pentti J. Tienari[27], David J. Stone[28,†], Karen E. Morrison[29], Pamela J. Shaw[30], Ammar Al-Chalabi[3], Robert H. Brown, Jr[31], Maura Brunetti[32], Andrea Calvo[33], Gabriele Mora[34], Marc Gotkine[35], Fawn Leigh[36], Ian Glass[5,6], Christopher E. Shaw[3,12], John E. Landers[31], Adriano Chiò[33,37,#], Thomas O. Crawford[38,#], Bradley N. Smith[3,#], Bryan J. Traynor[1,16,#]

[1]Neuromuscular Diseases Research Section, Laboratory of Neurogenetics, National Institute on Aging, National Institutes of Health, Bethesda, MD 20892, USA

[2]Cell Biology and Gene Expression Section, Laboratory of Neurogenetics, National Institute on Aging, National Institutes of Health, Bethesda, MD 20892, USA

[3]Maurice Wohl Clinical Neuroscience Institute, Institute of Psychiatry, Psychology and Neuroscience, King's College London, Camberwell, SE5 9NU, London, UK

[4]Department of Biology, Imam Abdulrahman bin Faisal University, Dammam, Saudi Arabia

[5]Department of Medicine, Division of Medical Genetics, University of Washington, Seattle, WA 98195, USA

[6]Department of Pediatrics, Division of Genetic Medicine, University of Washington, Seattle, WA and Seattle Children's Hospital, Seattle, WA 98105, USA

[7]Sobell Department of Motor Neuroscience and Movement Disorders, University College London, Institute of Neurology, London, UK

[8]Molecular Genetics Section, Laboratory of Neurogenetics, National Institute on Aging, National Institutes of Health, Bethesda, MD 20892, USA

[9]Department of Computer Science, University of Illinois at Urbana-Champaign, Urbana, IL 61801, USA

[10]Department of Neuroscience, Icahn School of Medicine at Mount Sinai, New York, NY 10029, USA

[11]Ronald M. Loeb Center for Alzheimer's Disease, Icahn School of Medicine at Mount Sinai, New York, NY 10029, USA

[12]UK Dementia Research Institute at King's College London, London, UK

[13]Computational Biology Core, Laboratory of Neurogenetics, National Institute on Aging, National Institutes of Health, Bethesda, MD 20892, USA

[14]Data Tecnica International, Glen Echo, MD 20812, USA

[15]Department of Pathology, Johns Hopkins University School of Medicine, Baltimore, MD 21205, USA

[16]Department of Neurology, Johns Hopkins University, Baltimore, MD 21287, USA

[17]Neurodegenerative Diseases Research Unit, Laboratory of Neurogenetics, National Institute of Neurological Disorders and Stroke, National Institutes of Health, Bethesda, MD 20892, USA

[18]Department of Anatomy, Physiology & Genetics, Uniformed Services University of the Health Sciences, Bethesda, MD 20814, USA

[19]The American Genome Center, Collaborative Health Initiative Research Program, Uniformed Services University of the Health Sciences, Bethesda, MD 20814, USA

[20]Istituto Auxologico Italiano, IRCCS, Department of Neurology-Stroke Unit and Laboratory of Neuroscience, Milan 20145, Italy

[21]Department of Pathophysiology and Transplantation, "Dino Ferrari" Center, Università degli Studi di Milano, Milan 20122, Italy

[22]Unit of Genetics of Neurodegenerative and Metabolic Diseases, Fondazione IRCCS Istituto Neurologico 'Carlo Besta', Milan 20133, Italy

[23]Centre for Motor Neuron Disease Research, Department of Biomedical Sciences, Faculty of Medicine and Health Sciences, Macquarie University, Sydney, New South Wales, Australia

[24]The University of Sydney, Brain and Mind Centre and Central Clinical School, Faculty of Medicine and Health, Camperdown, New South Wales, Australia

[25]School of Medical Sciences, University of New South Wales, Kensington, New South Wales, Australia

[26]Human Genetics Branch, National Institute of Mental Health, National Institutes of Health, Bethesda, MD 20892, USA

[27]Department of Neurology, Helsinki University Hospital and Translational Immunology Programme, Biomedicum, University of Helsinki, Helsinki FIN-02900, Finland

[28]Genetics and Pharmacogenomics, Merck & Co., Inc., West Point, PA 19486, USA

[29]Faculty of Medicine, University of Southampton, University Hospital Southampton NHS Foundation Trust, Southampton, UK

[30]Sheffield Institute for Translational Neuroscience, Department of Neuroscience, University of Sheffield, Sheffield S10 2HQ, UK

[31]Department of Neurology, University of Massachusetts Medical School, Worcester, MA 01605, USA

[32]Molecular Genetics Unit, Department of Clinical Pathology, A.S.O. O.I.R.M.-S. Anna, 10126 Turin, Italy

[33]'Rita Levi Montalcini' Department of Neuroscience, University of Turin, Turin, Italy

[34]ALS Center, ICS Maugeri, IRCCS, Milan, Italy

[35]Department of Neurology, The Agnes Ginges Center for Human Neurogenetics, Hadassah-Hebrew University Medical Center, Israel

[36]Department of Neurology, Seattle Children's Hospital, University of Washington, Seattle, WA 98105, USA

[37]AOU Città della Salute e della Scienza, Turin, Italy

[38]Departments of Neurology and Pediatrics, Johns Hopkins University, Baltimore, MD 21287, USA

[#] These authors contributed equally to this article

† Current address: Cerevel Therapeutics, Boston, MA 02116, USA

* Corresponding author. Email: ruth.chia@nih.gov

Abstract: *SPTLC1* encodes a critical subunit of serine palmitoyltransferase, the enzyme catalyzing the first and rate-limiting step in *de novo* sphingolipid biosynthesis, and mutations in this gene are known to cause *hereditary sensory autonomic neuropathy, type 1A*. Using exome sequencing, we identified a *de novo* variant in *SPTLC1* resulting in a p.Ala20Ser amino acid change in an individual diagnosed with juvenile-onset amyotrophic lateral sclerosis (ALS) and confirmed its pathogenicity by showing elevated plasma levels of neurotoxic deoxymethyl-sphinganine. A second case of juvenile-onset ALS arising again from a p.Ala20Ser mutation was later identified, confirming the association of *SPTLC1* with this form of motor neuron disease. We also found *SPTLC1* mutations in 0.34% of 5,607 ALS cases, and immunohistochemically confirmed the expression of SPTLC1 in spinal cord motor neurons, supporting their role in the pathogenesis of this fatal neurological disease. We corrected the toxicity of deoxymethyl-sphinganine in HEK293FT cells using L-serine supplementation. Our data broaden the phenotype associated with *SPTLC1* and suggest that nutritional supplementation with serine may be beneficial if instituted at an early stage among patients carrying mutations in *SPTLC1*.

Introduction

Amyotrophic lateral sclerosis (ALS, OMIM number 105400) is the third most common neurodegenerative disease in adults and is characterized by rapidly progressive paralysis leading to death due to respiratory failure within two to three years of symptom onset *(1)*. It is the most common adult-onset form of motor neuron disease, typically occurring in middle age or later. The number of ALS cases across the globe will increase to nearly 400,000 in 2040, predominantly due to population aging *(2)*. Approximately 10% of ALS is familial, whereas the remaining cases are classified as sporadic *(3)*.

Considerable progress has been made in unraveling the genetic architecture underlying familial ALS, and the genetic etiology of about two-thirds of familial ALS has been determined *(4, 5)*. In contrast, the genetic factors involved in the more common sporadic form of this fatal disorder are mostly unknown. Genome-wide association studies have identified only a handful of loci, many of which have proven difficult to replicate *(5)*. Our lack of knowledge concerning the pathogenesis of sporadic ALS hampers efforts to design disease-modifying interventions.

One possible explanation for the limited success of genome-wide association studies may be that *de novo* genetic variants underlie a small portion of sporadic ALS. Such mutations would not be readily detectable by genome-wide association owing to their recent occurrence and corresponding low frequency in the community as they have not yet had the opportunity to propagate. Spontaneously occurring mutations are a well-known cause of neurological and non-neurological conditions, such as neurofibromatosis type 1 *(6)* and Hirschsprung's disease *(7)*. Indeed, *de novo* mutations of the familial ALS genes, *FUS*, *SOD1*, and *VCP*, have been previously described in sporadic ALS cases *(8–10)*.

Here, we describe the exome sequencing of an affected individual diagnosed with juvenile-onset ALS, as well as DNA obtained from her unaffected parents and siblings, in an attempt to identify the genetic lesion responsible for the disease. We subsequently identified a second unrelated individual with juvenile-onset ALS carrying the same mutation. After identifying these underlying mutations, we further investigated if variation in the same gene occurred in adult-onset ALS cases.

Results

Exome sequencing identifies *SPTLC1* mutations in two juvenile ALS cases

We studied an American family (USALS#6, fig. 1A) in which the proband had been diagnosed with juvenile-onset ALS, and there was no family history of neurodegenerative disease. Our analysis identified two *de novo* variants that were present in the proband and not present in her parents or her healthy siblings, namely a p.Ala20Ser (chr9:94874844, C>A) heterozygous mutation in serine palmitoyltransferase long chain base subunit 1 (*SPTLC1*), and a p.Thr140insVal (chr4:120982056T>TCAC) non-frameshift insertion in mitotic arrest deficient 2 like 1 (*MAD2L1*). We did not identify any recessive coding changes in the proband.

Through the Genematcher program at GeneDx *(11)*, we identified a second individual also carrying a p.Ala20Ser amino acid change (USALS#7, fig. 1C). This amino acid shift arose from a mutation in an adjacent nucleotide compared to the proband of USALS#6 (chr9:94874843, G>T). She presented at the age of 10 with progressive skeletal muscle wasting, tongue fasciculations and wasting in the absence of sensory and autonomic deficits. This variant was also detected in 2% (n = 1 out of 49 reads) of the exome sequencing reads from her 61-year old unaffected father's saliva-derived DNA suggesting mosaicism. No other variants of unknown

significance were identified in the proband, and three paternal half-siblings and their children were reportedly unaffected.

Neither of the SPTLC1 p.Ala20Ser variants were present in 4,647 control subjects sequenced as part of the Alzheimer's disease sequencing project (ADSP), or in large online databases of human polymorphisms including the Genome Aggregation Database (gnomAD, non-neurological Finnish and non-Finnish European individuals, n = 60,541 individuals) and the Kaviar Genomic Variant database (Kaviar, n = 77,301 individuals).

Mutations in *SPTLC1* are a known cause of autosomal dominant, *hereditary sensory and autonomic neuropathy, type 1A* (HSAN1A, OMIM number 162400) *(12, 13)*. Interestingly, there is a previous report of a *de novo* p.Ser331Phe (chr9:94809543, C>T) mutation in *SPTLC1* in a young French girl presenting with a similar phenotype consisting of severe restriction of growth, cognitive impairment, hypotonia, amyotrophy, vocal cord paralysis, and respiratory failure *(14)*.

The full-length transcript carrying the p.Ala20Ser mutation is pathogenic

Computational analysis predicted that the p.Ala20Ser (chr9:94874844, C>A) mutation altered splicing of *SPTLC1* due to its proximity to the exon-intron border. In addition to the canonical ~400bp transcript, exon trap experiments identified a smaller ~300bp fragment in the proband that was not present in unaffected family members (fig. S1A). Cloning and sequencing confirmed that the larger fragment in the proband contained all of exon 2 and that ~25% of these transcripts contained the C>A mutation (fig. S1B). In contrast, the smaller fragment was produced by the complete omission of exon 2.

Western blot analysis performed using peripheral blood mononuclear cells obtained from the proband detected a single protein band of about 50 kD corresponding to the canonical SPTLC1 protein (fig. S1C). This band confirmed that the alternatively spliced variants of *SPTLC1* were not translated and suggested that the full-length transcript carrying the C>A transversion translating to p.Ala20Ser mutation at the protein level was responsible for the underlying pathogenic mechanism.

Elevated plasma deoxymethyl-sphinganine in the patient carrying the *de novo SPTLC1* mutation

The protein encoded by *SPTLC1* is an essential subunit of serine palmitoyltransferase, the enzyme that catalyzes the first and rate-limiting step in the *de novo* synthesis of sphingolipids *(15)*. This initial step normally involves the condensation of L-serine and activated fatty acid palmitoyl-CoA to form sphinganine. A characteristic feature of *SPTLC1* mutations associated with *hereditary sensory and autonomic neuropathy, type 1A* is a shift in substrate specificity of serine palmitoyltransferase to L-alanine and L-glycine leading to the formation of an atypical class of deoxy-sphingolipids *(16)*. The lack of a C1 hydroxyl group on these deoxy-sphingolipids means that they cannot be converted to complex sphingolipids nor degraded by the classic catabolic pathway, so instead they accumulate within cells *(16)*.

Abnormally elevated plasma levels of deoxy-sphingolipids is a known biomarker for pathogenic *SPTLC1* mutations *(16)*. Mass spectrometry demonstrated an abnormally high level of 1-deoxymethyl-sphinganine in the proband of the USALS#6 kindred carrying the p.Ala20Ser *SPTLC1* mutation that was not present in her unaffected parents, her unaffected siblings, or

control subjects (fig. 1B). These findings confirmed that this *de novo* mutation had abnormally altered the function of the SPTLC1 protein and was the likely cause of disease in this individual.

Immunohistological examination of spinal cord tissue

Immunohistological examination of spinal cord tissue obtained from a non-ALS control individual shows that SPTLC1 was highly expressed in motor neurons of the anterior horn (fig. 2 and S2). The location and morphology of these cells were consistent with alpha motor neurons of the dorsolateral motor nucleus. In contrast, the intensity and number of motor neurons staining with SPTLC1 were diminished in autopsy tissue obtained from a patient with sporadic ALS of unknown etiology and an ALS patient carrying a p.Arg445Gln mutation in SPTLC1. This staining pattern is consistent with motor neuron degeneration that has occurred during the disease process. Remaining motor neurons in the ALS patients did not show apparent signs of SPTLC1 protein aggregation or mislocalization.

Sequencing identifies *SPTLC1* mutations in adult-onset ALS

Next, we explored the occurrence of *SPTLC1* mutations in a more extensive series of 5,607 ALS cases. This screening identified seventeen novel mutations in 19 (0.34%) cases. These mutations were not present in exome sequence data of 4,647 control individuals sequenced as part of ADSP; occurred with a frequency less than 3.3×10^{-5} in large online databases of human polymorphisms consisting of 137,842 individuals (gnomAD and Kaviar); and were predicted to be damaging and conserved across multiple variant prediction algorithms (see Table 1, fig. 3 and S3). Table 2 lists the clinical features of the cases carrying the *SPTLC1* mutations.

The p.Ala305Thr variant in *SPTLC1* was found in three patients in a cohort of 1,646 patients with familial ALS. Only two out of 135,025 in-house or online subjects (ADSP, gnomAD, and Kaviar) carried this variant, and its presence was highly associated with the risk of developing ALS (Fisher p-value = 1.7×10^{-5}, odds ratio = 122.8, 95% confidence interval = 14.1 – 1,531.8).

Of the three individuals carrying p.Ala305Thr (see fig. S4 for pedigrees), one was part of an Australian kindred manifesting frontotemporal dementia (FTD) and ALS *(17)*. Within this family, the *SPTLC1* mutation was present in an individual diagnosed with ALS and was not found in the three individuals diagnosed with FTD or in one diagnosed with FTD-ALS. The second individual carrying the p.Ala305Thr was an American who presented with familial bulbar-onset ALS at the age of 76. DNA was not available from other family members. The third individual carrying the p.Ala305Thr variant was a 68-year-old patient diagnosed with ALS who was part of an ALS UK kindred. Available DNA showed two unaffected siblings (aged 66 and 65 years) to be carriers.

Interestingly, we detected a common haplotype in the three individuals carrying the p.Ala305Thr mutation extending across at least 43 kilobase pairs, suggesting this mutation originated from a common founder and that the three individuals are distantly related (Table S1). Overall, these genetic data point toward p.Ala305Thr being a rare, variably penetrant risk factor within the population.

Overall, we found mutations in *SPTLC1* in 0.34% of ALS cases (n = 19 out of 5,607 cases or 1 in 295 cases), meaning that it is a relatively rare cause of this fatal neurodegenerative disease. Nevertheless, gene burden analysis based on rare and damaging variants identified in these 5,607 cases (Tables 1 and 2) and in similarly filtered 60,541 non-neurological gnomAD

samples of Finnish and European ancestry supported an association with ALS (66 variants in population samples, one-sided Fisher test p-value = 7.5×10^{-5}).

Toxic sphingolipid metabolite induces mitochondrial changes in cellular models

Serum samples were not available from the ALS patients carrying the *SPTLC1* mutations, so it was not possible to confirm the presence of abnormal sphingolipid biochemistry. Instead, we sought to assess the pathogenicity of the *SPTLC1* mutations using cellular modeling. A fundamental advantage of this *in vitro* approach was that it enabled us to gauge the response to serine supplementation and to provide preliminary evidence as to whether patients carrying a specific mutation in *SPTLC1* may benefit from therapy with this naturally-occurring dietary amino acid.

To do this, we took advantage of previous work reporting that exposure of cells with deoxy-sphingolipids results in the loss of mitochondrial membrane potential *(18)*. We based our high-content assay on HEK293FT cell lines to ensure ease of implementation across laboratories and generation of rapid, reliable data. We opted not to employ induced pluripotent stem (iPS) cell lines for this assay due to the difficulty, time and expense required to establish such cells in a new laboratory, and due to the potential variability across laboratories.

We hypothesized that deoxymethyl-sphinganine, the deoxy-sphingolipid that was elevated in our p.Ala20Ser patient, would have a similar toxic effect on mitochondria. To test this, we used MitoTracker Red CMXRos, a fluorescent dye whose uptake is governed by membrane potential, to measure the effects of deoxymethyl-sphinganine treatment on HEK293FT cells. Treatment with 0.5 μM concentrations of deoxymethyl-sphinganine over 48

hours led to a significant decrease in Mitotracker labelling of mitochondria (fig. 4A and 4B). This experiment demonstrates that the toxic metabolite deoxymethyl-sphinganine can induce mitochondrial depolarisation in a concentration-dependent manner. Additionally, a significant decrease in the average mitochondrial area accompanied the loss of mitochondrial membrane potential. These changes in mitochondria morphology were not observed following 48-hour treatment with similar concentrations of sphinganine, a physiological product the levels of which were not changed in the proband who carried the *SPTLC1* p.Ala20Ser mutation (fig. 1B, S5A and S5B).

Mutations in *SPTLC1* induce mitochondrial changes in cellular models

We next used this high-content assay to test whether mutations in *SPTLC1* recapitulate our observed mitochondria phenotype. To this end, we overexpressed either wild-type *SPTLC1* or one of the following mutations: p.Ala20Ser, p.Cys133Trp, and p.Ala305Thr in HEK293FT cells. The p.Cys133Trp is a known cause of *hereditary sensory and autonomic neuropathy, type 1A*, and served as a positive control. We generated stable cells using lentivirus as transient overexpression using plasmids resulted in the formation of large aggregates and cell death. This approach resulted in cellular expression of SPTLC1 at levels ten times higher than that of endogenous SPTLC1 that was well tolerated by HEK293FT cells based on Mitotracker red staining and expression of ER stress markers (see fig. S5D-G).

Using our stable cell lines, we compared mitochondrial morphology between cells overexpressing wild-type SPTLC1 and mutant SPTLC1. Mitotracker uptake showed that the mitochondrial membrane potential and the average area was significantly decreased in all cells expressing mutant SPTLC1 when compared to cells overexpressing wild-type SPTLC1 (fig. 4).

Since mitochondrial membrane potential is fundamental for the generation of ATP, we next measured cellular ATP levels using the CellTiter-Glo luminescent assay. Consistent with our Mitotracker data, lower levels of ATP were observed in cells overexpressing mutant SPTLC1 compared to wild-type SPTLC1 (fig. 4).

L-serine normalizes mitochondrial changes induced by *SPTLC1* mutations in cellular models

Increasing the cellular concentration of L-serine has been proposed to mitigate the production of deoxy-sphingolipids by mutant SPTLC1 protein. From a translational perspective, we sought to determine if the addition of serine to our cellular model would ameliorate the detrimental effects of *SPTLC1* mutations.

Following treatment with 100 mM serine for 48 hours, there was no significant difference in the mitochondrial membrane potential or the mitochondrial area between wild-type and any of the mutant SPTLC1 cell lines (fig. 4C-D and 4F-G, 4I). Treatment with serine also led to a significant increase in ATP levels in each of the mutant lines (fig. 4E and 4H).

Using the same *in vitro* model system, we evaluated whether increased concentrations of glycine and L-alanine exacerbated the toxicity of mutant SPTLC1. A highly significant decrease in mitochondrial potential was observed following 48-hour treatment with 100 mM glycine in all mutant cell lines, as well as in the wild-type SPTLC1 cell line (fig. S6A). A decrease in mitochondrial potential was only observed in wild-type SPTLC1 cell lines following 48-hour treatment with 100 mM L-alanine (fig. S6B).

Discussion

We provide compelling genetic and biochemical data that mutations in *SPTLC1* are the cause of disease in two cases of juvenile-onset ALS. First, we found two different mutations leading to an Ala20Ser amino acid change in two affected individuals with similar motor neuron phenotypes. One affected individual carried a *de novo* variant that was not found in her healthy parents or siblings. In contrast, the second affected individual likely inherited their p.Ala20Ser variant in an autosomal dominant manner from her father, in whom we found low-level mosaicism. Neither mutation was present in our in-house control dataset or online databases of human polymorphisms, indicating it was a rare variant in ethnically diverse populations.

Second, mutations in this gene are already known to cause neurological disease with diverse phenotypes, and a *de novo* mutation involving the same gene has been previously reported to be associated with a clinical syndrome similar to that observed in our proband *(14)*.

Third, mass spectrometry analysis of plasma obtained from our affected index patient confirmed the presence of abnormal sphingolipid metabolites indicating that the observed mutation disrupts the function of the encoded enzyme leading to increased aberrant utilization of glycine as substrate. This biochemical pattern was consistent with the pattern previously reported to be the disease-causing mechanism in such patients *(16)*. We used an *in vitro* biochemical assay to confirm that the p.Ala20Ser mutation shifts substrate specificity leading to increased use of non-canonical glycine and alanine and no discernible change in serine utilization (see fig. S8).

Finally, we used immunohistochemistry to demonstrate that SPTLC1 is abundantly expressed within the motor neurons of healthy spinal cord tissue. Although SPTLC1 mutations are more commonly linked to a sensory and autonomic neurological phenotype, these data

support a role for this protein, and more generally sphingolipid metabolism, in motor neuron diseases such as ALS *(19)*.

We also provide genetic evidence that mutations in *SPTLC1* are a rare cause of adult-onset classical ALS. Key among these data was the discovery of three ALS patients, each of whom carried the same p.Ala305Thr variant. This variant was present only twice in ~270,000 control chromosomes. Interestingly, these three cases were geographically isolated (resident in the USA, the United Kingdom, and Australia), but shared the same haplotype across the *SPTLC1* locus suggesting that these individuals potentially share a common ancestral founder.

The alanine residue at position 305 lies within the pyridoxal 5'-phosphate-binding site and substrate-cofactor binding pocket, and protein structure modeling indicates that the change from non-polar alanine to the larger and more polar threonine may significantly alter molecular conformation as the protein is forced to accommodate the bulkier amino acid in a buried location (see fig. S7).

Though labeled as *hereditary sensory and autonomic neuropathy type 1A,* the phenotypes associated with mutations in *SPTLC1* are known to be diverse with patients manifesting various combinations of sensory loss, autonomic dysfunction, and motor weakness *(20)*. This clinical heterogeneity has been linked to the differing effects of each mutation on SPTLC1 enzyme-substrate preference *(16)*. We observed wide-ranging differences in substrate specificity across the mutations that we biochemically studied.

Adding to this complexity is the possibility that neuronal subtypes are differentially sensitive to distinct deoxysphingolipid species. Under this paradigm, the species of toxic sphingolipid generated by each mutation in the SPTLC1 enzyme and the relative sensitivity of

neuronal subtypes to those toxic species dictates whether sensory, autonomic, or motor symptoms dominate the clinical picture. Certain mutations lead to the accumulation of specific deoxysphingolipids that rapidly damage sensory and autonomic neurons, and give rise to juvenile and early adult-onset hereditary sensory autonomic neuropathy. In contrast, patients carrying the p.Ala305Thr variant only developed the disease after their sixth decade of life. It is possible that the *SPTLC1* mutations associated with late-onset ALS result in a more gradual aggregation of different toxic sphingolipids that lead to motor neuron degeneration later in life.

Perturbed sphingolipid metabolism underlies many common neurological disorders, such as Niemann-Pick disease and Gaucher disease *(21)*, and may play a role in the pathogenesis of Alzheimer's disease *(22)*. Sphingolipid metabolism has also been directly implicated in motor neuron degeneration *(23)*. For example, Tay-Sachs disease (also known as GM2 gangliosidosis, a form of sphingolipidosis) is an autosomal recessive genetic disorder due to hexosaminidase A deficiency that is prevalent among Ashkenazi Jews and French Canadians *(24)*. Patients with partial deficiency of hexosaminidase A enzyme activity may have clinical manifestations mimicking ALS *(25)*. Accumulation of ceramides and cholesterol esters also occurs within the spinal cords of ALS patients and a *SOD1* transgenic mouse model of ALS *(26)*. Hyperlipidemia has also been shown to be a significant risk factor for developing ALS *(27)*.

Our data suggest that consideration should be given to screening patients diagnosed with ALS for *SPTLC1* mutations, especially as dietary supplementation with serine may be beneficial if instituted at an early stage in the disease course *(28)*. Serine is a non-essential amino acid that is widely available as an inexpensive nutritional supplement. A 10% serine-enriched diet reduced neurotoxic deoxysphingolipid plasma levels both in transgenic mice expressing the p.C133W *SPTLC1* mutation and in human patients diagnosed with *hereditary sensory and autonomic*

neuropathy, type 1A (HSAN1) (28). Furthermore, a safety trial involving twenty ALS patients demonstrated that up to 30 grams of oral serine per day are well-tolerated over six months of treatment and that this polar amino acid is actively transported across the blood-brain barrier *(29)*. We are hopeful that serine supplementation might have similar beneficial effects in SPTLC1-related ALS as that observed for HSAN1.

ALS patients participating in the clinical trial of serine supplementation failed to show significant neurological improvement, though the relative rarity of *SPTLC1* mutations (1 in 295 cases in our study) make it unlikely that the study enrolled any mutation carriers. This negative outcome suggests that improved selection criteria are needed to tailor therapies to the underlying molecular defect. Under this precision medicine paradigm, only ALS patients carrying pathogenic SPTLC1 mutations would receive serine supplementation. Abnormal deoxysphingolipid plasma metabolites could act as a diagnostic or selection biomarker to confirm the toxicity of *SPTLC1* mutations before enrollment, and also as a marker of target engagement after commencing treatment.

Our cell-based assays in which we modeled *SPTLC1* mutations support our proposition that serine supplementation may benefit this patient group. Each of the three mutations that we evaluated using this high content system demonstrated decreased cell viability across multiple assays, and all three of these mutant cell lines returned to regular activity upon the addition of serine.

Our approach to these *in vitro* experiments capitalized on prior knowledge showing *SPTLC1* mutations result in acute calcium handling abnormalities and mitochondrial dysfunction *(18)*. We applied these assays as a means to gauge the pathogenicity of mutations and to model the potential effect of serine supplementation in patients. We provide a detailed description of

the methodology used in these assays in the supplementary material so that other groups can apply these procedures to assess other *SPTLC1* mutations.

Only a small number of patients diagnosed with ALS are likely to carry pathogenic *SPTLC1* mutations and to benefit from serine supplementation. However, the dire prognosis associated with ALS, together with the immediate availability of a well-tolerated and inexpensive targeted therapy (i.e., serine), alters the risk-benefit ratio and provides an early opportunity to test the precision medicine approach in neurodegenerative disease. Nutritional supplementation has proven to be remarkably effective in other forms of ALS: high dose oral vitamin B_2 (riboflavin) slows and even halts neurological progression in Brown-Vialetto-Van Laere cases *(30)*, a rare subtype of ALS arising from mutations in the riboflavin pathway *(31, 32)*.

Our study has limitations. Due to the nature of spontaneous and sporadic mutations, we could not show segregation with the disease within extended kindreds. The lack of large pedigrees has generally hampered the ALS genetics field, and in part arises from the poor survival associated with the disease. The availability of a robust biomarker based on the measurement of the responsible toxic species partially mitigates these concerns and provides additional evidence of pathogenicity. Furthermore, though mutations in *SPTLC1* are an infrequent cause of ALS, our work implicates a novel pathway in ALS, namely sphingolipid metabolism. The discovery of a new gene may have an outsized effect on our understanding of diseases, even when those mutations are rare. For example, the identification of *TREM2* mutations in a handful of patients diagnosed with Alzheimer's disease highlighted the role of microglia and inflammation in that form of neurodegenerative disease and paved the way for

innovative approaches to therapy *(33)*. The discovery of GBA mutations had a similar impact on Parkinson's disease research *(34)*.

In conclusion, our data broaden the phenotype associated with mutations in *SPTLC1* and indicate that nutritional supplementation with serine may improve the toxic effect of abnormal sphingolipid metabolites if instituted at an early stage in the disease.

Materials and Methods

Patients

The proband of the USALS#6 kindred had presented with spastic diplegia and growth retardation at five years of age (see fig. 1A for pedigree). By age 20, she had quadriplegia with marked muscle atrophy, brisk lower limb reflexes, tongue fasciculations and weakness, dysarthria, mild cognitive dysfunction, and respiratory failure requiring tracheostomy and ventilation. Repeated neurophysiological testing did not show evidence of sensory or autonomic dysfunction. She was diagnosed with ALS based on the revised El Escorial criteria *(35)*. There was no family history of ALS or any other neurodegenerative diseases. A detailed clinical description of this case is available in the supplementary material. DNA was obtained from the proband of USALS#6, as well as her unaffected parents and her three unaffected siblings.

The proband of the USALS#7 family developed predominantly lower limb muscle weakness at the age of 8 (see fig. 1C for pedigree). By age 11 she had difficulty climbing stairs. Tongue fasciculations were first observed at age 12. At the age of 15, she had marked muscle atrophy with diminished body weight (body mass index z-score below -7), tongue fasciculations and wasting (see movie S1), and generalized limb weakness that was worse proximally . Recurrent neurological testing failed to identify sensory abnormalities. On examination, she

demonstrated bilateral scapula winging, brisk asymmetric ankle reflexes with diminished knees and upper limbs reflexes, a florid Gower's sign (see movie S2), and an exaggerated lumbar lordosis. School performance began to decline at the age of 15. An extensive endocrinology workup for her failure to gain weight was unremarkable. DNA was obtained from the proband of USALS#7 and her unaffected parents.

For subsequent mutational screening of *SPTLC1*, an additional 5,607 DNA samples were obtained from individuals diagnosed with ALS. Of these, 1,208 cases underwent exome sequencing at the NIH, 1,274 cases underwent genome sequencing at the Broad Institute or The American Genome Center, 650 cases underwent Sanger sequencing of the *SPTLC1* gene at the NIH, 1,170 samples underwent exome sequencing at the University of Massachusetts as part of the FALS Sequencing Consortium, and 1,305 samples underwent genome sequencing as part of the UK MNDA sequencing effort that is part of Project MinE *(36)*.

Control data consisted of 4,647 neurologically healthy U.S. individuals who had undergone exome sequencing as part of the Alzheimer's Disease Sequencing Project (dbGaP, accession number phs000572.v7.p4). Table S2 provides the clinical details of the case and control samples.

All subjects provided written informed consent for genetic analysis according to the Declaration of Helsinki, and the study was approved by the Institutional Review Board of the National Institutes of Health (protocol number AG-03-N329).

Generation of stable cell lines expressing wild type and mutant SPTLC1

Single site mutations resulting in amino acid substitutions at p.A20S, p.C133W and p.A305T were introduced into a plasmid containing the human *SPTLC1* open reading frame tagged with

FLAG-myc at the N-terminal (Origene Technologies Inc., NM_006415) using the QuikChange II XL Site-Directed Mutagenesis kit (Agilent Technologies Inc.) following the manufacturer's recommendations. All plasmids were sequenced-verified. Table S3 lists the primers used for mutagenesis.

The *SPTLC1* open reading frame was then subcloned into pLenti-C-Myc-DDK-P2A-Puro lentiviral transfer plasmid (Origene) between the *Sgf1* and *MluI* cloning sites. Lentiviruses were produced with third generation packaging plasmids (pMDLg/pRRE and pRSV-Rev, Addgene) and envelope plasmid (pMD2.G, Addgene) as previously described *(37)*. Viral titers were estimated using the qPCR Lentiviral Titration kit (Applied Biological Materials Inc.).

HEK293FT were transfected with wild-type or mutant lentivirus transfer plasmid (titer range between 6–35x10^8 genome copies per ml). Transcduced cells stably expressing SPTLC1 were selected with extended growth in 0.5 ug/ml puromycin (Thermo Fisher). Cell lines expressing SPTLC1 levels most similar across wild-type and mutants were selected for downstream biochemical and cellular assays. Expression levels of SPTLC1 in each cell line were determined by Western blot by detecting the FLAG-tagged protein using normalized to loading protein GAPDH (Abcam PLC).

Exome sequencing of the USALS#6 and USALS#7 pedigrees

DNA from the USALS#6 pedigree was enriched using Illumina TruSeq kit according to the manufacturer's protocol (version 1.0, Illumina Inc.), and the captured DNA underwent 100 base pair, paired-end sequencing on a HiSeq 2000 sequencing system (Illumina). Sequence alignment and variant calling were performed against the reference human genome (Genome Reference Consortium Human build 37) using the Genome Analysis Toolkit (GATK, version 3.3). PCR

duplicates were removed before variant calling using Picard software. We generated an average of 7.6 gigabases (range, 6.9 to 8.1) of sequence data for the samples of the USALS#6 kindred, providing adequate coverage across the exome (average percentage of the exome with 10 or more reads in all samples = 91.5%, range, 90.4 to 92.6%).

For the proband and parents of the USALS#7 pedigree, the exonic regions and flanking splice junctions of the genome were captured using the IDT xGen Exome Research Panel (version 1.0). The captured DNA underwent 100bp or greater paired-end sequencing on an Illumina system. Sequence reads were aligned to the reference human genome (build 37), and analyzed for sequence variants using a custom-developed analysis tool. Additional sequencing technology and variant interpretation protocol has been previously described *(38)*. The general assertion criteria for variant classification are publicly available on the GeneDx ClinVar submission page.

Data generation for follow-up cohorts

For the follow-up samples used at the Laboratory of Neurogenetics, exome sequence data for 1,208 cases were generated in the same manner as the data generated for the USALS#6 pedigree. These data, along with the data for the 4,647 control subjects of ADSP downloaded from dbGaP, were aligned in the same manner as the data generated for the USALS#6 pedigree. Genome sequence data for 1,274 cases were generated using 150 base pair, paired-end sequencing on an Illumina X10 sequencer following TruSeq library preparation. Sequence reads were aligned to the reference human genome build 37 using the GATK Toolkit. We sequenced the fifteen coding exons and flanking introns of the *SPTLC1* gene (NM_006415.3) in the 650 ALS cases of the follow-up cohort using the BigDye Terminator v3.1 chemistry (Thermo Fisher Scientific Inc.),

run on a 3730xl DNA Analyzer (Thermo Fisher), and analyzed using *Sequencher* software (version 4.2, Gene Codes). Table S3 lists the PCR primer sequences and conditions.

Sequence data for the 1,170 samples of the FALS Sequencing Consortium and 1,305 samples of the King's College London effort were processed in a similar manner. Assembly and processing of whole-genome sequence data of the UK MNDA sporadic ALS samples were performed as previously published *(39)*.

SPTLC1 transcript analysis

RNA was extracted from lymphoblastoid cells using Trizol (Thermo Fisher), reverse transcribed using SuperScript III First-Strand Synthesis SuperMix (Thermo Fisher), followed by PCR amplification using the primer pair CGGAGCAGTGGGTTCTGG (exon1F) and CCTCTGGGTCCACAAGTCC (exon5R) with FastStartPCR Master Mix (Sigma Aldrich). Amplified PCR products were assessed on 2% E-Gel EX Agarose Gels (Thermo Fisher), cloned using the TOPO TA Cloning® Kits for Sequencing (Thermo Fisher) according to the manufacturer's protocol, and plasmids were extracted using QIAprep Spin Miniprep Kit (Qiagen). Plasmid and TA-cloned inserts were Sanger sequenced using the universal M13 forward primer.

Measurement of sphingolipid levels

Sphingolipids were extracted from plasma using methanol extraction *(40)*. Chromatographic separation was performed on an Acquity Ultra Performance Liquid Chromatography (UPLC) system (Waters Corp.) by injecting 5 ul of the samples into an Aquity UPLC Charged Surface Hybrid C_{18} column (Waters). The mobile phase consisted of 0.2% volume/volume (v/v) of

formic acid in both water (A), and acetonitrile (B). A gradient elution was used over 5.5 minutes with a flow rate of 0.4 ml per minute as follows: 0–3 minutes = 10–80% B; 3–4 minutes = 80–90% B; 4–5 minutes = 90–50% B; and 5–5.5 minutes = 50–10% B. The column temperature was maintained at 40°C. The sphingolipids were then detected in a Xevo TQ-S triple quadrupole-mass spectrometer (Waters) using the multiple reaction monitoring method. Recognizing the variability in mass spectroscopy data across different centers, we have provided the raw data generated by these experiments in the supplementary material.

Acquired data were analyzed using *MassLynx* software (version 4.1, Waters). Calibration equations for the sphingolipids were obtained by plotting response against concentration (ng/mL). The equation showed good linearity over the 1 ng to 3,000 ng range (see Table S4 for raw mass spectrometry data).

Western blotting

Western blot was performed as previously described *(41)*. We used the following primary antibodies at the indicated dilutions: mouse anti-Flag (1:5,000, Sigma-Aldrich), rabbit anti-SPTLC1 (1:1,000, Sigma-Aldrich), rabbit anti-SPTLC2 (1:1000, LifeSpan BioSciences Inc.), and rabbit anti-GAPDH (Sigma-Aldrich).

Immunopurification of SPTLC1 protein complex

SPTLC1-FLAG proteins were immuno-purified from HEK293FT cells that were stably expressing SPTLC1. Cells were lysed in lysis buffer (50 mM HEPES, pH8.0, 1 mM EDTA, 0.1% (w/v) sodium monolaurate, phosphatase (Thermo Fisher) and protease inhibitor (Roche AG), and membrane proteins were further solubilized by sonication for fifteen seconds at 50%

power and 50% pulsation for a total of 45 seconds. The lysate was clarified by centrifugation at 21,000g for five minutes at 4°C to remove large cellular debris followed by immunoprecipitation with EZview Red Anti-Flag M2 Affinity Gel (Sigma-Aldrich) as previously described *(41)*.

Purified SPTLC1-FLAG was quantified against a bovine serum albumin protein standard curve (BSA, Thermo Fisher) ran on an SDS-PAGE gel and transferred to a nitrocellulose membrane (Bio-rad). Membrane was stained with Revert Total Protein Stain (LI-COR), and imaged on an Odyssey CLx imaging system. Interaction of SPTLC2 with SPTLC1-FLAG was confirmed by Western blot showing that the purified serine palmitoyltransferase complex was likely functional.

Photometric serine palmitoyltransferase enzymatic assay

Condensation of serine and palmitoyl-CoA by serine palmitoyltransferase enzyme produces 3-ketodihydrosphingosine and releases both carbon dioxide and free coenzyme A (CoA). This photometric assay measures the amount of free CoA released that is reactive to 5,5'-dithiobis-2-nitrobenzoic acid (DTNB, Thermo Fisher) reflective of the enzymatic activity of serine palmitoyltransferase.

This assay was adapted from and shown to be comparable to radioactive assays measuring radiolabeled 3-ketodihydrosphingosine *(42)*. Triplicate wells were assayed per 100ng of purified wild-type or mutant SPTLC1 proteins, and per amino acid tested. The product of the reaction was measured at 412 nm at the zero time point and every two minutes for up to one hour. Varying concentrations of CoA, in place of purified SPTLC1-FLAG protein, were included as a standard to build the calibration curve for the estimation of CoA released from the serine

palmitoyltransferase enzymatic reaction. Estimated amounts of CoA produced per nanogram of SPTLC1-FLAG protein were plotted over time for each amino acid.

In silico protein modelling

The structure of SPTLC1 was predicted using *I-TASSER*, and the most reliable match was selected. The generated model was based on the *S. paucimobilis* serine palmitoyltransferase structure (protein data bank accession number: 2JG2) *(43, 44)*. Heterodimeric complex (SPTLC1 and SPTLC2) modeling was generated using the *COTH* and *SPRING* online tools *(45)*. Hydrophobicity, electrostatics, interface residues, and mutational analysis modeling were performed using *PyMOL* (version 2.0, Schrödinger).

Immunohistochemistry of spinal cord

Immunohistochemistry was performed by Histoserv on lumbar spinal cords obtained from a neurologically healthy control, from a sporadic ALS case, and from an ALS case known to carry the p.Arg445Gln *SPTLC1* mutation. Formalin-fixed, paraffin-embedded blocks were sectioned to 5 um thickness and were stained with primary anti-SPTLC1 antibody (Sigma-Aldrich) at 1:50 dilution overnight at 4°C and counter-stained with hematoxylin. Tiled images of full spinal cord sections were recorded using a color camera on a Zeiss Wide Angle microscope using a 20x/0.8 Plan Apochromat objective.

Quantification of *BiP* and spliced *XBP-1* mRNA

Quantification of BiP and spliced XBP-1 mRNA was used as a readout of ER stress as previously described *(46)*. Non-transduced HEK293FT cells and cells overexpressing wild-type

and mutant SPTLC1 were cultured in 12-well plates for twenty-four hours using Minimum Essential Medium (MEM, Thermo Fisher) supplemented with 10% FBS. Four hours before collection, non-transduced cells were treated with 5 mM thapsigargin (Abcam). Total mRNA was then extracted using TRIzol (Thermo Fisher) according to the manufacturer's protocol. RNA was then converted into cDNA using the SuperScript III First-Strand Synthesis Supermix (Thermo Fisher).

Quantitative RT-PCR was performed using Power SYBR Green PCR master mix (Thermo Fisher) to measure the levels of BiP and spliced *XBP-1* mRNA and the housekeeper gene *β-actin*. Table S3 lists the primer pairs. All samples were run in quadruplicate on a QuantStudio 6 Flex Real-Time PCR System (Thermo Fisher). Expression levels of spliced *XBP-1* were calculated using the delta-delta Ct method following normalization to *β-actin*.

Treatment with metabolite or amino acids

Metabolic products of serine palmitoyltransferase activity (Avanti Polar Lipids Inc.) were reconstituted in methanol (AmericanBio) to a stock concentration of 10 mM. Two hours after plating, the cells were treated with sphinganine, deoxy-sphinganine, or deoxymethyl-sphinganine to a working concentration range between 0.1 mM and 10 mM for 24 hours.

L-serine, L-glycine, and L-alanine were dissolved in MEM media. Where required, cells were treated two hours after plating at final concentrations ranging from 10 mM to 1000 mM for 48 hours.

Assessment of mitochondrial morphology and ATP levels

Mitochondrial potential and area were measured using MitoTracker Red CMXRos (Thermo Fisher). Mitochondria in live cells were incubated with 100 nM MitoTracker Red at 37°C for one

hour, then fixed with 4% paraformaldehyde (Thermo Fisher) followed by washing with PBS prior to being imaged at either 20x or 40x on a CellInsight CX7 LZR High Content Analysis instrument (Thermo Fisher). Mitochondrial parameters were assessed automatically using the built-in compartmental analysis protocol (*HCS Studio - Compartment Analysis*, version 4). A minimum of six wells was scanned for each condition, and 400 cells were analyzed in each well.

To quantify the levels of cellular ATP, the cells were lysed with CellTiter-Glo Luminescent Cell Viability reagent (Promega Corp.) and luminescence was measured using a SpectraMax M5 microplate reader (Molecular Devices LLC.).

Statistical analyses

Analysis of the USALS#6 kindred

Paternity and maternity in the USALS#6 kindred were confirmed using identity-by-descent analysis as implemented within the PLINK software toolset (version 1.9). Exome data were reviewed to ensure that members of USALS#6 pedigree did not carry pathogenic mutations in known ALS-related genes (*ALS2, CHCHD10, CHMP2B, DCTN1, FUS*, *KIF5A, MATR3*, *NEK1, OPTN, PFN1, SETX*, *SOD1*, *SPG11, SQSTM1*, *TARDBP*, *TBK1, TUBA4A, UBQLN2*, *VAPB, VCP*, and *VEGFA*). The USALS#6 kindred members were also confirmed not to carry the *C9orf72* repeat expansion using repeat-primed PCR *(47)*.

Data from USALS#6 were analyzed to identify single nucleotide variants and insertions/deletions (indels) that were present in the affected child, but not present in either parent (i.e., *de novo*). *De novo* mutations underlying a rare disease such as ALS are unlikely to be present in the general population. For this reason, we removed variants present in the gnomAD database (version 2.1, covering 51,592 non-Finnish European and 8,949 Finnish

European individuals without neurological disease), or in the Kaviar Genomic Variant database (version September 23, 2015, covering 77,301 individuals). Next, synonymous, intronic and intergenic changes were filtered from the variant list using *ANNOVAR* annotation software (August 11, 2016 version).

Sanger sequencing using customized primers (Operon Technologies Inc.) was performed to confirm the presence and absence of the variants in relevant samples of the USALS#6 kindred as described below.

Analysis of SPTLC1 in follow-up cohorts

We selected *SPTLC1* variants identified in the follow-up cohorts if: (a) they were not present in the 4,647 control ADSP subjects; (b) they had a frequency less than 3.3×10^{-5} in online databases of human polymorphisms *(4)*. These included the 51,592 European and 8,949 Finnish non-neurological individuals in gnomAD, and the 77,301 samples in Kaviar; (c) they altered the protein-coding sequence; and (d) they were designated as 'damaging' according to four out of five prediction algorithms (FATHMM, M-CAP, MetaLR, MetaSVM and VEST3) recently identified as the most reliable prediction tools *(48)*; were identified as “stop gain” or “frameshift”; or had a dbscSNV adaptive boosting score higher than 0.6 in the case of splice site mutations *(49)*. Sanger sequencing using customized primers was performed as described above to confirm the presence of the variants in relevant samples.

Association analysis for p.Ala305Thr was performed using a two-sided Fisher test as implemented in R. As control data, we used allele counts from gnomAD for Finnish and non-Finnish European samples without neurological diseases (n = 53,075 Finnish and non-Finnish European individuals without neurological disease), and from Kaviar (n = 77,031 individuals).

Due to lower coverage of this variant, the number of samples in gnomAD was lower than what was used for filtering and gene burden testing (https://gnomad.broadinstitute.org/variant/9-94809966-C-T?dataset=gnomad_r2_1_non_neuro).

Gene burden testing of *SPTLC1* was performed using publicly available control data as implemented in the *TRAPD* software package *(50)*. This script performs a one-sided Fisher's exact test to determine if there is a higher burden of qualifying variants in cases as compared to controls for a tested gene. It was not possible to include covariates to control for population stratification in the analysis as only summary-level statistics were available for the gnomAD dataset, so instead, we restricted our control dataset to known Finnish and non-Finnish European individuals. As case data, we used filtered data for the 5,454 patients diagnosed with ALS as described above. As control data, we used variant data downloaded from gnomAD for Finnish and non-Finnish European samples without neurological diseases (n = 60,541 individuals). High-quality variants in the control data were filtered in the same manner as the case dataset.

Analysis of readout from high-throughput mitochondrial assay

Statistical analyses for all mitochondrial assays measuring mitochondrial morphology and ATP levels were performed using *Prism* (version 6.0, GraphPad Software). We measured a minimum of six wells for each condition, and all assays were performed at least twice. Unpaired t-test with Welch's correction was performed for experiments with two groups. For experiments with more than two groups, comparison to a single control group was assessed using one-way ANOVA with Dunnett's multiple comparison test applied. Two-way ANOVA with Tukey's *posthoc* test was used to calculate statistical significance in instances where two factors, such as treatment

and cell type, were present in the experimental design. Comparisons were considered statistically significant if the p-value was less than 0.05.

References

1. L. P. Rowland, N. A. Shneider, Amyotrophic Lateral Sclerosis. *N. Engl. J. Med.* 344, 1688–1700 (2001).
2. K. C. Arthur, A. Calvo, T. R. Price, J. T. Geiger, A. Chiò, B. J. Traynor, Projected increase in amyotrophic lateral sclerosis from 2015 to 2040. *Nat. Commun.* 7, 12408 (2016).
3. A. Chiò, A. Calvo, L. Mazzini, R. Cantello, G. Mora, C. Moglia, L. Corrado, S. D'Alfonso, E. Majounie, A. Renton, F. Pisano, I. Ossola, M. Brunetti, B. J. Traynor, G. Restagno, On behalf of PARALS, Extensive genetics of ALS: A population-based study in Italy. *Neurology* 79, 1983–1989 (2012).
4. R. Chia, A. Chiò, B. J. Traynor, Novel genes associated with amyotrophic lateral sclerosis: diagnostic and clinical implications. *Lancet Neurol.* 17, 94–102 (2018).
5. A. E. Renton, A. Chiò, B. J. Traynor, State of play in amyotrophic lateral sclerosis genetics. *Nat. Neurosci.* 17, 17–23 (2014).
6. M. Littler, N. E. Morton, Segregation analysis of peripheral neurofibromatosis (NF1). *J. Med. Genet.* 27, 307–310 (1990).
7. S. M. Ivanchuk, S. M. Myers, C. Eng, L. M. Mulligan, De novo mutation of GDNF, ligand for the RET/GDNFR-alpha receptor complex, in Hirschsprung disease. *Hum. Mol. Genet.* 5, 2023–2026 (1996).
8. M. D. Alexander, B. J. Traynor, N. Miller, B. Corr, E. Frost, S. McQuaid, F. M. Brett, A. Green, O. Hardiman, "True" sporadic ALS associated with a novel SOD-1 mutation. *Ann. Neurol.* 52, 680–683 (2002).
9. A. Chiò, A. Calvo, C. Moglia, I. Ossola, M. Brunetti, L. Sbaiz, S.-L. Lai, Y. Abramzon, B. J. Traynor, G. Restagno, A de novo missense mutation of the FUS gene in a "true" sporadic ALS case. *Neurobiol. Aging* 32, 553.e23–553.e26 (2011).
10. T. Ayaki, H. Ito, H. Fukushima, T. Inoue, T. Kondo, A. Ikemoto, T. Asano, A. Shodai, T. Fujita, S. Fukui, H. Morino, S. Nakano, H. Kusaka, H. Yamashita, M. Ihara, R. Matsumoto, J. Kawamata, M. Urushitani, H. Kawakami, R. Takahashi, Immunoreactivity of valosin-containing protein in sporadic amyotrophic lateral sclerosis and in a case of its novel mutant. *Acta Neuropathol. Commun.* 2 (2014), doi:10.1186/s40478-014-0172-0.
11. N. Sobreira, F. Schiettecatte, D. Valle, A. Hamosh, GeneMatcher: a matching tool for connecting investigators with an interest in the same gene. *Hum. Mutat.* 36, 928–930 (2015).
12. K. Bejaoui, C. Wu, M. D. Scheffler, G. Haan, P. Ashby, L. Wu, P. de Jong, R. H. Brown Jr, SPTLC1 is mutated in hereditary sensory neuropathy, type 1. *Nat. Genet.* 27, 261–262 (2001).
13. J. L. Dawkins, D. J. Hulme, S. B. Brahmbhatt, M. Auer-Grumbach, G. A. Nicholson, Mutations in SPTLC1, encoding serine palmitoyltransferase, long chain base subunit-1, cause hereditary sensory neuropathy type I. *Nat. Genet.* 27, 309–312 (2001).
14. A. Rotthier, J. Baets, E. De Vriendt, A. Jacobs, M. Auer-Grumbach, N. Lévy, N. Bonello-Palot, S. S. Kilic, J. Weis, A. Nascimento, M. Swinkels, M. C. Kruyt, A. Jordanova, P. De

Jonghe, V. Timmerman, Genes for hereditary sensory and autonomic neuropathies: a genotype-phenotype correlation. *Brain* 132, 2699–2711 (2009).

15. K. Hanada, Serine palmitoyltransferase, a key enzyme of sphingolipid metabolism. *Biochim. Biophys. Acta* 1632, 16–30 (2003).

16. A. Penno, M. M. Reilly, H. Houlden, M. Laurá, K. Rentsch, V. Niederkofler, E. T. Stoeckli, G. Nicholson, F. Eichler, R. H. Brown Jr, A. von Eckardstein, T. Hornemann, Hereditary sensory neuropathy type 1 is caused by the accumulation of two neurotoxic sphingolipids. *J. Biol. Chem.* 285, 11178–11187 (2010).

17. C. Dobson-Stone, A. A. Luty, E. M. Thompson, P. Blumbergs, W. S. Brooks, C. L. Short, C. D. Field, P. K. Panegyres, J. Hecker, J. A. Solski, I. P. Blair, J. M. Fullerton, G. M. Halliday, P. R. Schofield, J. B. J. Kwok, Frontotemporal dementia-amyotrophic lateral sclerosis syndrome locus on chromosome 16p12.1-q12.2: genetic, clinical and neuropathological analysis. *Acta Neuropathol.* 125, 523–533 (2013).

18. E. R. Wilson, U. Kugathasan, A. Y. Abramov, A. J. Clark, D. L. H. Bennett, M. M. Reilly, L. Greensmith, B. Kalmar, Hereditary sensory neuropathy type 1-associated deoxysphingolipids cause neurotoxicity, acute calcium handling abnormalities and mitochondrial dysfunction in vitro. *Neurobiol. Dis.* 117, 1–14 (2018).

19. F. Schmitt, G. Hussain, L. Dupuis, J.-P. Loeffler, A. Henriques, A plural role for lipids in motor neuron diseases: energy, signaling and structure. *Front. Cell. Neurosci.* 8, 25 (2014).

20. G. A. Nicholson, in GeneReviews, M. P. Adam, H. H. Ardinger, R. A. Pagon, S. E. Wallace, L. J. H. Bean, K. Stephens, A. Amemiya, Eds. (University of Washington, Seattle, Seattle (WA), 2002).

21. F. Sabourdy, L. Astudillo, C. Colacios, P. Dubot, M. Mrad, B. Ségui, N. Andrieu-Abadie, T. Levade, Monogenic neurological disorders of sphingolipid metabolism. *Biochim. Biophys. Acta* 1851, 1040–1051 (2015).

22. N. J. Haughey, V. V. R. Bandaru, M. Bae, M. P. Mattson, Roles for dysfunctional sphingolipid metabolism in Alzheimer's disease neuropathogenesis. *Biochim. Biophys. Acta 1801*, 878–886 (2010).

23. A. Henriques, V. Croixmarie, D. A. Priestman, A. Rosenbohm, S. Dirrig-Grosch, E. D'Ambra, M. Huebecker, G. Hussain, C. Boursier-Neyret, A. Echaniz-Laguna, A. C. Ludolph, F. M. Platt, B. Walther, M. Spedding, J.-P. Loeffler, J.-L. Gonzalez De Aguilar, Amyotrophic lateral sclerosis and denervation alter sphingolipids and up-regulate glucosylceramide synthase. *Hum. Mol. Genet.* 24, 7390–7405 (2015).

24. R. Myerowitz, N. D. Hogikyan, Different mutations in Ashkenazi Jewish and non-Jewish French Canadians with Tay-Sachs disease. *Science* 232, 1646–1648 (1986).

25. H. Mitsumoto, R.J. Sliman, I.A. Schafer, C.S. Sternick, B. Kaufman, A. Wilbourn, S.J. Horwitz, Motor neuron disease and adult hexosaminidase A deficiency in two families: evidence for multisystem degeneration. Ann Neurol 17, 378–385 (1985).

26. R. G. Cutler, W. A. Pedersen, S. Camandola, J. D. Rothstein, M. P. Mattson, Evidence that accumulation of ceramides and cholesterol esters mediates oxidative stress-induced death of motor neurons in amyotrophic lateral sclerosis. *Ann. Neurol.* 52, 448–457 (2002).

27. S. Bandres-Ciga, A. J. Noyce, G. Hemani, A. Nicolas, A. Calvo, G. Mora, ITALSGEN Consortium, International ALS Genomics Consortium, P. J. Tienari, D. J. Stone, M. A. Nalls, A. B. Singleton, A. Chiò, B. J. Traynor, Shared polygenic risk and causal inferences in amyotrophic lateral sclerosis. *Ann. Neurol.* 85, 470–481 (2019).

28. K. Garofalo, A. Penno, B. P. Schmidt, H.-J. Lee, M. P. Frosch, A. von Eckardstein, R. H. Brown, T. Hornemann, F. S. Eichler, Oral L-serine supplementation reduces production of neurotoxic deoxysphingolipids in mice and humans with hereditary sensory autonomic neuropathy type 1. *J. Clin. Invest.* 121, 4735–4745 (2011).

29. T. D. Levine, R. G. Miller, W. G. Bradley, D. H. Moore, D. S. Saperstein, L. E. Flynn, J. S. Katz, D. A. Forshew, J. S. Metcalf, S. A. Banack, P. A. Cox, Phase I clinical trial of safety of L-serine for ALS patients. *Amyotroph. Lateral Scler. Frontotemporal Degener.* 18, 107–111 (2017).

30. A. R. Foley, M. P. Menezes, A. Pandraud, M. A. Gonzalez, A. Al-Odaib, A. J. Abrams, K. Sugano, A. Yonezawa, A. Y. Manzur, J. Burns, I. Hughes, B. G. McCullagh, H. Jungbluth, M. J. Lim, J.-P. Lin, A. Megarbane, J. A. Urtizberea, A. H. Shah, J. Antony, R. Webster, A. Broomfield, J. Ng, A. A. Mathew, J. J. O'Byrne, E. Forman, M. Scoto, M. Prasad, K. O'Brien, S. Olpin, M. Oppenheim, I. Hargreaves, J. M. Land, M. X. Wang, K. Carpenter, R. Horvath, V. Straub, M. Lek, W. Gold, M. O. Farrell, S. Brandner, R. Phadke, K. Matsubara, M. L. McGarvey, S. S. Scherer, P. S. Baxter, M. D. King, P. Clayton, S. Rahman, M. M. Reilly, R. A. Ouvrier, J. Christodoulou, S. Züchner, F. Muntoni, H. Houlden, Treatable childhood neuronopathy caused by mutations in riboflavin transporter RFVT2. *Brain* 137, 44–56 (2014).

31. P. Green, M. Wiseman, Y. J. Crow, H. Houlden, S. Riphagen, J.-P. Lin, F. L. Raymond, A.-M. Childs, E. Sheridan, S. Edwards, D. J. Josifova, Brown-Vialetto-Van Laere syndrome, a ponto-bulbar palsy with deafness, is caused by mutations in c20orf54. *Am. J. Hum. Genet.* 86, 485–489 (2010).

32. J. O. Johnson, J. R. Gibbs, A. Megarbane, J. A. Urtizberea, D. G. Hernandez, A. R. Foley, S. Arepalli, A. Pandraud, J. Simón-Sánchez, P. Clayton, M. M. Reilly, F. Muntoni, Y. Abramzon, H. Houlden, A. B. Singleton, Exome sequencing reveals riboflavin transporter mutations as a cause of motor neuron disease. *Brain* 135, 2875–2882 (2012).

33. R. Guerreiro, A. Wojtas, J. Bras, M. Carrasquillo, E. Rogaeva, E. Majounie, C. Cruchaga, C. Sassi, J. S. K. Kauwe, S. Younkin, L. Hazrati, J. Collinge, J. Pocock, T. Lashley, J. Williams, J.-C. Lambert, P. Amouyel, A. Goate, R. Rademakers, K. Morgan, J. Powell, P. St George-Hyslop, A. Singleton, J. Hardy, Alzheimer Genetic Analysis Group, TREM2 variants in Alzheimer's disease. *N. Engl. J. Med.* 368, 117–127 (2013).

34. V. Berge-Seidl, L. Pihlstrøm, J. Maple-Grødem, L. Forsgren, J. Linder, J. P. Larsen, O.-B. Tysnes, M. Toft, The GBA variant E326K is associated with Parkinson's disease and explains a genome-wide association signal. *Neurosci. Lett.* 658, 48–52 (2017).

35. B. R. Brooks, R. G. Miller, M. Swash, T. L. Munsat, El Escorial revisited: Revised criteria for the diagnosis of amyotrophic lateral sclerosis. *Amyotroph. Lateral Scler. Other Motor Neuron Disord.* 1, 293–299 (2000).

36. Project MinE ALS Sequencing Consortium, Project MinE: study design and pilot analyses of a large-scale whole-genome sequencing study in amyotrophic lateral sclerosis. *Eur. J. Hum. Genet.* 26, 1537–1546 (2018).

37. N. Pilpel, N. Landeck, M. Klugmann, P. H. Seeburg, M. K. Schwarz, Rapid, reproducible transduction of select forebrain regions by targeted recombinant virus injection into the neonatal mouse brain. *J. Neurosci. Methods* 182, 55–63 (2009).

38. K. Retterer, J. Juusola, M. T. Cho, P. Vitazka, F. Millan, F. Gibellini, A. Vertino-Bell, N. Smaoui, J. Neidich, K. G. Monaghan, D. McKnight, R. Bai, S. Suchy, B. Friedman, J. Tahiliani, D. Pineda-Alvarez, G. Richard, T. Brandt, E. Haverfield, W. K. Chung, S. Bale, Clinical application of whole-exome sequencing across clinical indications. *Genet. Med.* 18, 696–704 (2016).

39. C. Raczy, R. Petrovski, C. T. Saunders, I. Chorny, S. Kruglyak, E. H. Margulies, H.-Y. Chuang, M. Källberg, S. A. Kumar, A. Liao, K. M. Little, M. P. Strömberg, S. W. Tanner, Isaac: ultra-fast whole-genome secondary analysis on Illumina sequencing platforms. *Bioinformatics* 29, 2041–2043 (2013).

40. A. H. Merrill Jr, M. C. Sullards, J. C. Allegood, S. Kelly, E. Wang, Sphingolipidomics: high-throughput, structure-specific, and quantitative analysis of sphingolipids by liquid chromatography tandem mass spectrometry. *Methods* 36, 207–224 (2005).

41. R. Chia, S. Haddock, A. Beilina, I. N. Rudenko, A. Mamais, A. Kaganovich, Y. Li, R. Kumaran, M. A. Nalls, M. R. Cookson, Phosphorylation of LRRK2 by casein kinase 1α regulates trans-Golgi clustering via differential interaction with ARHGEF7. *Nat. Commun.* 5, 5827 (2014).

42. M. F. Rütti, S. Richard, A. Penno, A. von Eckardstein, T. Hornemann, An improved method to determine serine palmitoyltransferase activity. *J. Lipid Res.* 50, 1237–1244 (2009).

43. J. Yang, R. Yan, A. Roy, D. Xu, J. Poisson, Y. Zhang, The I-TASSER Suite: protein structure and function prediction. *Nat. Methods* 12, 7–8 (2015).

44. B. A. Yard, L. G. Carter, K. A. Johnson, I. M. Overton, M. Dorward, H. Liu, S. A. McMahon, M. Oke, D. Puech, G. J. Barton, J. H. Naismith, D. J. Campopiano, The structure of serine palmitoyltransferase; gateway to sphingolipid biosynthesis. *J. Mol. Biol.* 370, 870–886 (2007).

45. A. Guerler, B. Govindarajoo, Y. Zhang, Mapping monomeric threading to protein-protein structure prediction. *J. Chem. Inf. Model.* 53, 717–725 (2013).

46. A. van Schadewijk, E. F. A. van't Wout, J. Stolk, P. S. Hiemstra, A quantitative method for detection of spliced X-box binding protein-1 (XBP1) mRNA as a measure of endoplasmic reticulum (ER) stress. *Cell Stress Chaperones* 17, 275–279 (2012).

47. A. E. Renton, E. Majounie, A. Waite, J. Simón-Sánchez, S. Rollinson, J. R. Gibbs, J. C. Schymick, H. Laaksovirta, J. C. van Swieten, L. Myllykangas, H. Kalimo, A. Paetau, Y. Abramzon, A. M. Remes, A. Kaganovich, S. W. Scholz, J. Duckworth, J. Ding, D. W. Harmer, D. G. Hernandez, J. O. Johnson, K. Mok, M. Ryten, D. Trabzuni, R. J. Guerreiro, R. W. Orrell, J. Neal, A. Murray, J. Pearson, I. E. Jansen, D. Sondervan, H. Seelaar, D. Blake, K. Young, N. Halliwell, J. B. Callister, G. Toulson, A. Richardson, A. Gerhard, J. Snowden,

D. Mann, D. Neary, M. A. Nalls, T. Peuralinna, L. Jansson, V.-M. Isoviita, A.-L. Kaivorinne, M. Hölttä-Vuori, E. Ikonen, R. Sulkava, M. Benatar, J. Wuu, A. Chiò, G. Restagno, G. Borghero, M. Sabatelli, ITALSGEN Consortium, D. Heckerman, E. Rogaeva, L. Zinman, J. D. Rothstein, M. Sendtner, C. Drepper, E. E. Eichler, C. Alkan, Z. Abdullaev, S. D. Pack, A. Dutra, E. Pak, J. Hardy, A. Singleton, N. M. Williams, P. Heutink, S. Pickering-Brown, H. R. Morris, P. J. Tienari, B. J. Traynor, A hexanucleotide repeat expansion in C9ORF72 is the cause of chromosome 9p21-linked ALS-FTD. *Neuron* 72, 257–268 (2011).

48. D. Anderson, T. Lassmann, A phenotype centric benchmark of variant prioritisation tools. *NPJ Genom Med* 3, 5 (2018).

49. X. Jian, X. Liu, In Silico Prediction of Deleteriousness for Nonsynonymous and Splice-Altering Single Nucleotide Variants in the Human Genome. *Methods Mol. Biol.* 1498, 191–197 (2017).

50. M. H. Guo, L. Plummer, Y.-M. Chan, J. N. Hirschhorn, M. F. Lippincott, Burden Testing of Rare Variants Identified through Exome Sequencing via Publicly Available Control Data. *Am. J. Hum. Genet.* 103, 522–534 (2018).

51. Z. S. Nasreddine, N. A. Phillips, V. Bedirian, S. Charbonneau, V. Whitehead, I. Collin, J. L. Cummings, H. Chertkow, The Montreal Cognitive Assessment, MoCA: A Brief Screening Tool For Mild Cognitive Impairment. *J. Am. Geriatr. Soc.* 53, 695–699 (2005).

52. A. Kertesz, W. Davidson, H. Fox, Frontal behavioral inventory: diagnostic criteria for frontal lobe dementia. *Can. J. Neurol. Sci.* 24, 29–36 (1997).

53. E. Mioshi, S. Hsieh, S. Savage, M. Hornberger, J. R. Hodges, Clinical staging and disease progression in frontotemporal dementia. *Neurology* 74, 1591–1597 (2010).

Acknowledgements: We thank the patients and their families for their participation in our research. We also thank Kirsty McWalter and GeneDx for their assistance. This study used DNA samples, genotype data, and clinical data from the NINDS Repository at Coriell, the New York Brain Bank-The Taub Institute, Columbia University, Department of Veterans Affairs Biorepository Brain Bank (grant #BX002466), the Baltimore Longitudinal Study of Aging (BLSA), the Johns Hopkins University Alzheimer's Disease Research Center (NIH grant P50AG05146), the NICHD Brain and Tissue Bank for Developmental Disorders at the University of Maryland, the MRC London Neurodegenerative Diseases Brain Bank, Kings College London, Denmark Hill, London, UK, and the Alzheimer's Disease Sequencing Project (www.niagads.org/adsp/content/acknowledgement-statement for more details). Samples used in this research were, in part, obtained from the U.K. MND Collections funded by the MND Association and the Wellcome Trust. We would also like to thank Peter R. Schofield, William S. Brooks, Elizabeth M. Thompson, Peter Blumbergs, Cathy L. Short, Colin D. Field, Peter K. Panegyres and Jane Hecker for their assistance in collecting samples from the Australian kindred.

Funding: This work was supported in part by the Intramural Research Programs of the NIH, National Institute on Aging (Z01-AG000949-02), and NINDS (ZIA-NS03154). The work was also funded by the Packard Center for ALS Research at Hopkins, the ALS Association, the Muscular Dystrophy Association, the Italian Ministry of Health (RF-2016-02362405), the Italian Ministry of Education, University and Research (Progetti di Ricerca di Rilevante Interesse Nazionale, PRIN, grant n. 2017SNW5MB), the Joint Programme - Neurodegenerative Disease Research (JPND, Brain-Mend projects) granted by Italian Ministry of Education, University and

Research, and by the European Community's Health Seventh Framework Programme (FP7/2007–2013, grant agreements no. 259867 and 278611), by the National Institute of Neurological Disorders and Stroke (NIH grant number R35 NS097261), and by the Collaborative Health Initiative Research Program. This study was performed under the Department of Excellence grant of the Italian Ministry of Education, University and Research to the 'Rita Levi Montalcini' Department of Neuroscience, University of Torino, Italy. Additional funding was also provided by the Motor Neurone Disease Association (MNDA), the Medical Research Council, the Medical Research Foundation (MRF), the Van Geest Foundation, The Psychiatry Research Trust of the Institute of Psychiatry, Guy's and St. Thomas' Charity and the Noreen Murray Foundation, the Sigrid Juselius Foundation, the UK Dementia Research Institute, the National Health and Medical Research Council of Australia (1095215, 1092023), and through the following funding organisations under the aegis of JPND: United Kingdom, Medical Research Council (MR/L501529/1; MR/R024804/1). This work was supported by the UK Dementia Research Institute which is funded by the Medical Research Council, Alzheimer's Society and Alzheimer's Research UK. Ammar Al-Chalabi is supported by the National Institute for Health Research (NIHR) Maudsley Biomedical Research Centre. Carol Dobson-Stone is supported by the Australian National Health and Medical Research Council (NHMRC) Boosting Dementia Research Leadership Fellowship 1138223 and by the University of Sydney. John B. Kwok is supported by NHMRC Dementia Research Team Grant 1095127.

Author contributions: *Sample Collection, Preparation, and Clinical Evaluation:* O.P., J.T., D.E.M, The International ALS Genomics Consortium; The ITALSGEN Consortium; the FALS

Consortium, Project MinE, I.B., C.D-S., J.B.K., R.H.B., A.C., G.M., A.C., T.C., C.E.S., M.G., B.N.S. and B.J.T..

Performed Experiments and Data Analysis: J.O.J., R.C., R.K., Y.A., F.F., A.E.R., H.A.P., S.D.T., N.A., J.R.G., J.D., M.A.N., C.D-S, M.N., C.L.D., S.W.S., M.S.S., S.A., I.G., F.L., J.E.L., B.N.S., A.C., T.C., and B.J.T.. *Scientific Planning and Direction:* R.C., R.K., J.E.L., A.C., T.C., B.J.T.. *Initial Manuscript Preparation:* R.C., R.K., J.E.L., A.C., T.C., B.N.S., B.J.T..

Competing interests: Pentti Tienari, Andrew B. Singleton, and Bryan J. Traynor hold US, Canadian and European patents on the clinical testing and therapeutic intervention for the hexanucleotide repeat expansion in C9orf72. Adriano Chiò serves on scientific advisory boards for Biogen Idec, Cytokinetics, Italfarmaco, and Neuraltus. Ammar Al-Chalabi reports consultancies for Biogen Idec, Cytokinetics Inc, OrionPharma, Chronos Therapeutics, and Mitsubishi-Tanabe Pharma. The other authors report no competing interests.

Data and materials availability: Alzheimer's Disease Sequencing Project (ADSP): https://www.niagads.org/adsp/content/home. Database of Genotypes and Phenotypes (dbGaP): https://www.ncbi.nlm.nih.gov/gap. Genome Aggregation Database (gnomAD): https://gnomad.broadinstitute.org. Haplotype Reference Consortium (HRC): www.haplotype-reference-consortium.org. Kaviar Genomic Variant Database: http://db.systemsbiology.net/kaviar/. ANNOVAR: annovar.openbioinformatics.org. Clustal Omega: www.ebi.ac.uk/Tools/msa/clustalo/. GATK: http://www.broadinstitute.org/gsa/wiki/index.php/Home_Page. HCS Studio: https://www.thermofisher.com/us/en/home/life-science/cell-analysis/cellular-imaging/high-

content-screening/high-content-screening-instruments/hcs-studio-2.html. I-TASSER (including *COTH* and *SPRING* algorithms): https://zhanglab.ccmb.med.umich.edu/I-TASSER. MassLynx: http://www.waters.com/waters/en_US/MassLynx-Mass-Spectrometry-Software-/nav.htm?cid=513164&locale=en_US. Picard: http://broadinstitute.github.io/picard. PLINK: https://www.cog-genomics.org/plink/1.9/. Prism: https://www.graphpad.com/scientific-software/prism/. PyMOL: pymol.org. R: https://www.r-project.org. Sequencher: http://genecodes.com. TRAPD: https://github.com/mhguo1/TRAPD. Further requests for resources and reagents should be directed to the Lead Contact, Ruth Chia (ruth.chia@nih.gov), Laboratory of Neurogenetics, NIA, NIH, 35 Convent Drive, Room 1A-1000, Bethesda, MD 20892, USA. Phone: (301) 451-7606. Fax: (301) 451-7295.

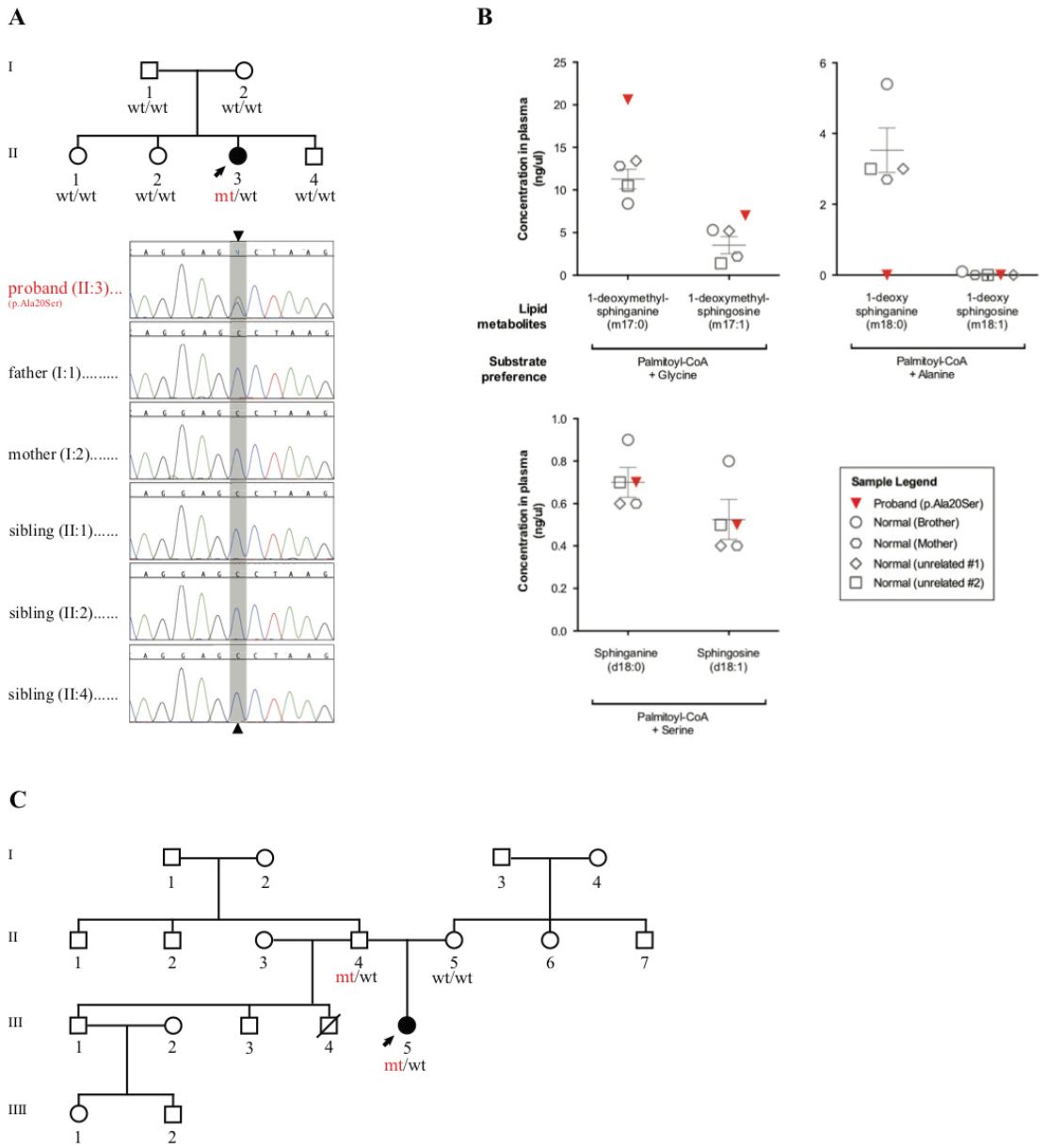

Fig. 1. *De novo* mutation of *SPTLC1* in a case of juvenile-onset ALS.

(A) Pedigree of family USALS#6. The mutant p.A20S allele in *SPTLC1* is indicated by *mt*, whereas wild-type alleles are indicated by *wt*. The arrow indicates the proband. Corresponding chromatograms showing mutant and wild-type alleles are as indicated. **(B)** Plasma analysis of the proband and healthy controls (unaffected mother, unaffected brother, and two unrelated healthy individuals). Proband had ~1.8 times higher levels of 1-deoxymethyl-sphinganine and 1-

deoxymethyl-sphingosine compared to the healthy controls. Utilization of L-alanine by the serine palmitoyltransferase complex produces 1-deoxysphinganine (m18:0) and 1-deoxysphingosine (m18:1), whereas the use of L-glycine yields 1-deoxymethyl-sphinganine (m17:0) and 1-deoxymethyl-sphingosine (m17:1). Collectively, these non-canonical metabolites are called deoxysphingoid bases. The nomenclature in brackets describes the number of hydroxyl groups (m for mono- and d for di-), followed by the number of carbons, and the number following ":" indicates the number of double bonds in the carbon backbone. **(C)** Pedigree of family USALS#7. The p.Ala20Ser mutation observed in the proband was found in 2% of exome sequencing reads from her unaffected father. Fig. S1 shows the effect of the p.Ala20Ser mutation on splicing and fig. S8 shows the effect on substrate utilization, demonstrating increased use of non-canonical glycine and alanine, and no apparent change in serine utilization.

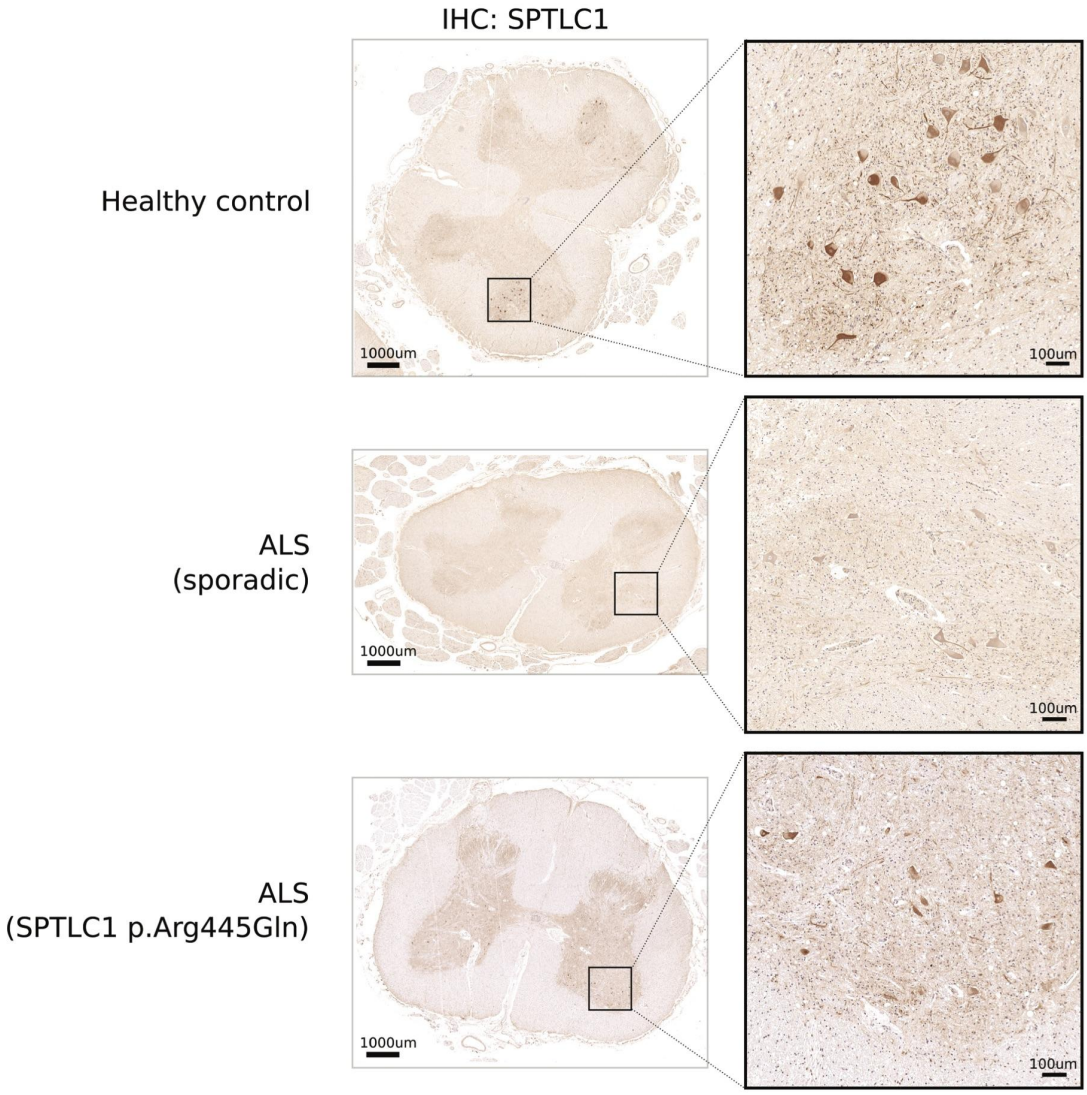

Fig. 2. Lumbar spinal cord tissue immunostained for SPTLC1 and counterstained with hematoxylin and eosin.

The control spinal cord (top panel) exhibits SPLTC1 immunoreactivity in the lamina IX motor neurons of the anterior horns. The spinal cord from a subject with sporadic ALS (middle panel)

exhibits weaker immunoreactivity in the same region consistent with a decrease in the number and size of surviving motor neurons. The surrounding healthy cells display normal staining. The spinal cord from an ALS case carrying the p.Arg445Gln mutation in SPTLC1 (bottom panel) shows a similar pattern of staining. Tiled images were taken at 20x magnification and stitched together with a 5% overlap between each image. Insets show enlargements of the boxed regions. Scale bars represent 50 um. Images are representative images of two sections cut from the same formalin-fixed, paraffin-embedded block of the same spinal cord region and stained on separate days. Fig. S2 shows the validation of the SPTLC1 antibody used for immunohistochemistry.

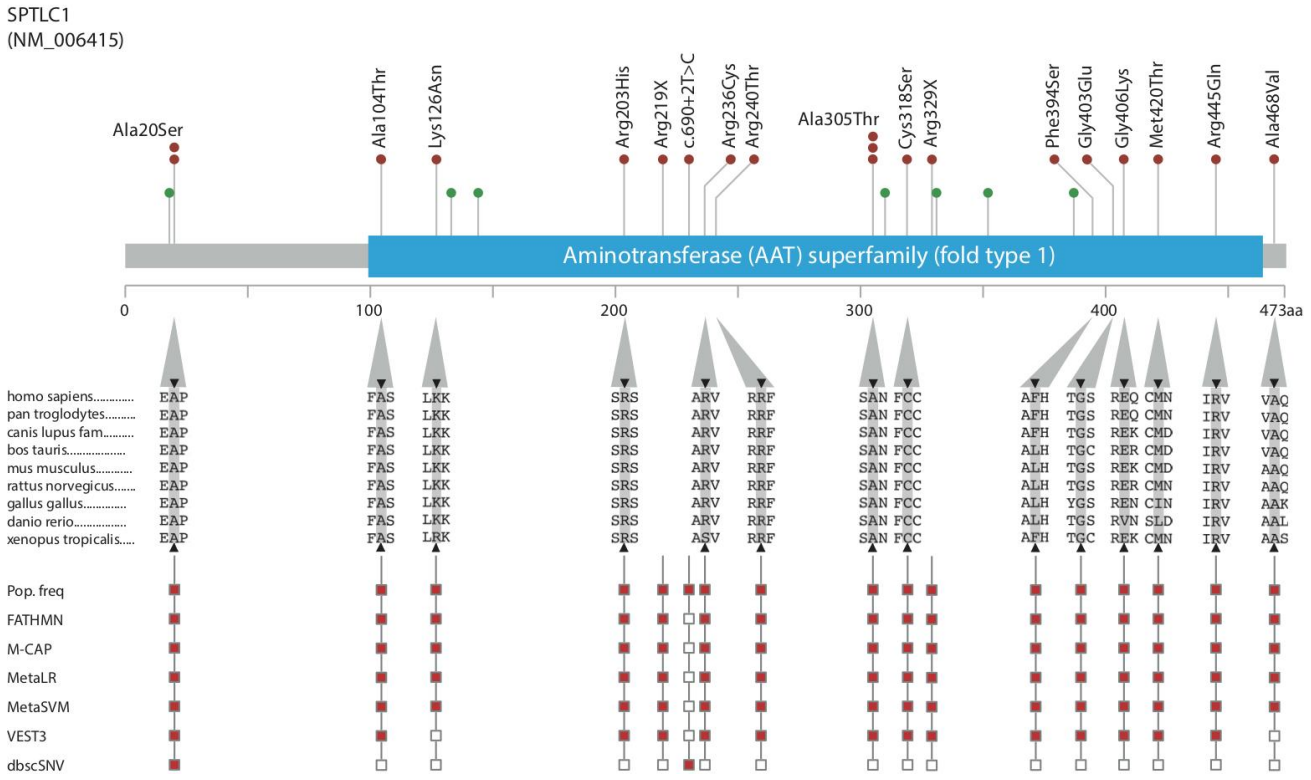

Fig. 3. Distribution of *SPTLC1* mutations detected in ALS patients.

The top panel is a graphical representation showing the domains of *SPTLC1*. Mutations detected in ALS cases are indicated in red, and mutations previously described to cause *hereditary sensory autonomic neuropathy, type 1A* are shown in green. The p.Ala305Thr variant was found in three ALS patients, the p.Ala20Ser was found in two ALS patients, and the other variants were found in single cases of ALS. The middle panel shows the conservation of amino acid residue across species generated using the Clustal Omega online tool. The bottom panel portrays population frequency data and functional predictions of the mutations. A red filled square means that a variant met criteria. Fig. S3, S4, and S7 show the corresponding chromatograms, pedigrees, and the location of mutations in the *SPTLC1* protein structure.

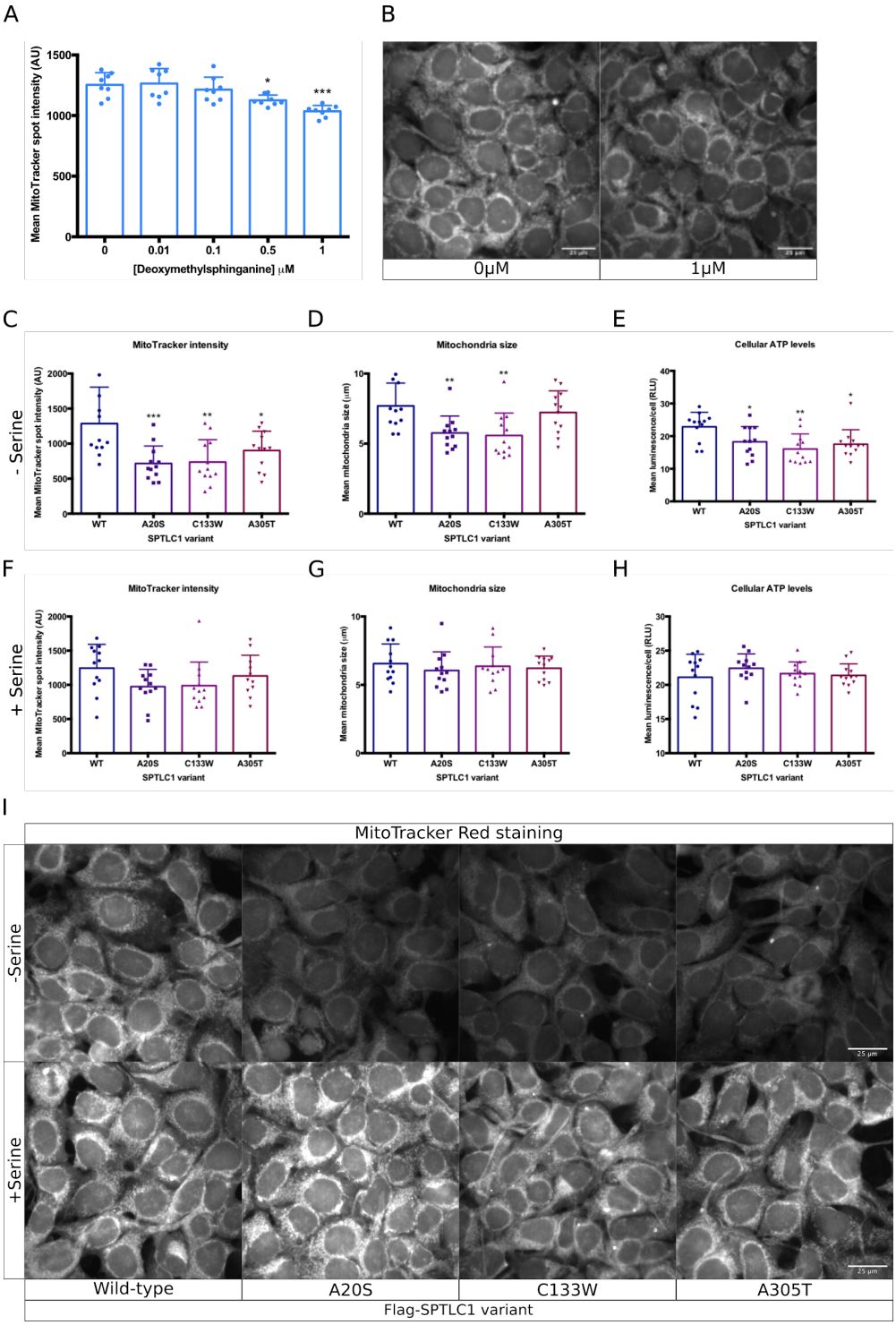

Fig. 4. Deoxymethylsphinganine and *SPTLC1* mutations promote mitochondrial dysfunction in HEK293FT cells

(A) Deoxymethylsphinganine lipid promoted loss of mitochondrial membrane potential in HEK293FT cells treated with increasing concentrations of deoxymethylsphinganine as measured using Mitotracker red. Statistical comparison to untreated cells was performed using a one-way ANOVA with Dunnett's *posthoc* test applied. Error bars represent standard deviation (SD), and significance was indicated as follows; *, $p<0.05$; ***, $p<0.001$. **(B)** Representative images from the CX7 LZR high-content analysis instrument showing decreased mitochondria staining of HEK293FT cells by Mitotracker red following treatment with 1μM deoxymethylsphinganine. **(C)** Mutations in *SPTLC1* resulted in decreased Mitotracker spot intensity (left graph) and area (center graph) representing the loss of mitochondria membrane potential and decreased mitochondria size. Mutations also led to decreased cellular ATP levels as measured by Cell-Glo reagent. Statistical comparison was performed to cells overexpressing Flag wild-type SPTLC1. **(D)** Treatment with 400 μM L-serine rescued mitochondrial abnormalities in cells overexpressing mutant SPTLC1. Cellular ATP levels (right graph) were also restored. **(E)** Representative image from CX7 LZR high-content analysis instrument of Mitotracker staining in wild-type and mutant SPTLC1 cells with and without treatment with 400 μM L-serine. Fig. S5 shows the treatment with sphingosine and the levels of SPTLC1 expression with lentivirus transfection. Fig. S6 demonstrates the effect of treatment with glycine and L-alanine. Each assay was performed two to four times, with eight to twelve wells per condition, and measurement was made on a minimum of 200 cells per well.

Table 1. *SPTLC1* mutations identified in ALS cases

SNP information		No. cases	Population frequency		Prediction and conservation algorithms		
			gnomAD	HRC	Prediction	Conservation	dbscSNV
9:94843196C>T	p.Ala104Thr	1	$1.1x10^{-5}$	0	damaging	conserved	NA
9:94842347C>G	p.Lys126Asn	1	0	0	damaging	not conserved	NA
9:94821543C>T	p.Arg203His	1	$1.1x10^{-5}$	0	damaging	conserved	NA
9:94821496G>A	p.Arg219X	1	$2.2x10^{-5}$	0	damaging	conserved	NA
9:94821459A>G	c.690+2T>C	1	0	0	NA	conserved	0.994
9:94817761G>A	p.Arg236Cys	1	0	0	damaging	not conserved	NA
9:94817749G>A	p.Arg240Cys	1	$1.1x10^{-5}$	0	damaging	conserved	NA
9:94809966C>T	p.Ala305Thr	3	$1.1x10^{-5}$	0	damaging	conserved	NA
9:94809927A>T	p.Cys318Ser	1	$1.1x10^{-5}$	0	damaging	conserved	NA
9:94809550G>A	p.Arg329X	1	$1.1x10^{-5}$	0	damaging	conserved	0.15
9:94800603A>G	p.Phe394Ser	1	0	0	damaging	conserved	NA
9:94800576C>T	p.Gly403Glu	1	0	0	damaging	conserved	NA
9:94800568C>T	p.Glu406Lys	1	0	0	damaging	conserved	NA
9:94797161A>G	p.Met420Thr	1	0	0	damaging	conserved	NA
9:94794835C>T	p.Arg445Gln	1	$2.2x10^{-5}$	0	damaging	conserved	NA
9:94794766G>A	p.Ala468Val	1	$1.1x10^{-5}$	0	damaging	conserved	NA
9:94794610A>-	p.Tyr509X	1	0	0	damaging	conserved	NA

Variant position is in build 19; amino acid change is based on the canonical transcript NP_006406, except for p.Tyr509X which is based on NP_001268232; No. cases, number of ALS cases carrying the variant; only variants with frequency less than $3.3x10^{-5}$ are shown (Chia et al, 2018); gnomAD, frequency shown is the maximum in either the Finnish or the non-Finnish European populations (non-neurological samples, version 2.1); HRC, Haplotype Reference Consortium (version 1); 'damaging' means the variant is designated as such by four out of five prediction algorithms consisting of FATHMM, M-CAP, MetaLR, MetaSVM and VEST3 *(48)*; 'conserved' means the position is considered as such by the GERP++, phastCons100way_vertebrate, phyloP100way_vertebrate, and SiPhy_29way algorithms; dbscSNV adaptive boosting score greater than 0.6 indicates a deleterious splice mutation *(49)*; NA, not available.

Table 2. Demographic and clinical features of patients diagnosed with ALS carrying *SPTLC1* mutations

Sample and mutation		Clinical and demographic features						
Sample	*Mutation*	*Sex*	*Age*	*Onset*	*Type*	*C9orf72*	*Sensory/ autonomic*	*Country*
ND13443	p.Ala104Thr	M	55	spinal	sporadic	no	none	USA
ALS1054	p.Lys126Asn	F	66	spinal	familial	no	none	Italy
ND12175	p.Arg203His	M	38	spinal	sporadic	no	none	USA
A14LIALS68	p.Arg219X	M	49	spinal	sporadic	no	none	Finland
A14LIALS349	c.690+2T>C	M	57	spinal	familial	yes	none	Finland
B555	p.Arg236Cys	M	51	spinal	sporadic	no	NA	Italy
SLA2010-83	p.Arg240Cys	M	73	bulbar	sporadic	no	none	Italy
ND10247	p.Ala305Thr	M	76	bulbar	familial	no	none	USA
AUS145-010335	p.Ala305Thr	F	58	NA	familial	no	NA	Australia
ALS0039	p.Ala305Thr	M	64	spinal	familial	no	none	UK
SLA2011-105	p.Cys318Ser	M	58	spinal	sporadic	no	none	Italy
UKS1	p.Arg329X	M	62	spinal	sporadic	no	none	UK
UKS2	p.Phe394Ser	M	54	spinal	sporadic	no	none	UK
SLA2014-383	p.Gly403Glu	F	75	bulbar	sporadic	no	none	Italy
A356	p.Glu406Lys	F	52	spinal	sporadic	no	NA	Italy
ND10984	p.Met420Thr	M	52	spinal	sporadic	no	none	USA
VABT110002	p.Arg445Gln	M	72	spinal	sporadic	no	none	USA
ALS0260	p.Ala468Val	M	81	spinal	sporadic	no	none	Israel
UKS3	p.Tyr509X	F	56	Mixed	sporadic	no	none	UK

Mutation description is based on the canonical NM_006415 transcript, except for p.Tyr509X which is based on NM_001281303.1; M refers to male and F to female; age refers to age at onset; onset refers to site where symptoms manifested initially; *C9orf72* refers to the pathogenic repeat expansion in that gene; country refers to population of origin of the sample. All patients carrying an *SPTLC1* mutation were of European-ancestry; NA means not available; samples starting with ND are available from the NINDS Repository at the Coriell Institute for Medical Research.